

# 1 Duration and nature of the end-Cryogenian (Marinoan) glaciation

2 <sup>1</sup>Anthony R. Prave, <sup>2</sup>Daniel J. Condon, <sup>3</sup>Karl Heinz Hoffmann, <sup>2</sup>Simon Tapster, and <sup>4</sup>Anthony  
3 **E. Fallick**

4 <sup>1</sup>*Department of Earth and Environmental Sciences, University of St Andrews, St Andrews, KY16*  
5 *9AL, UK*

6 <sup>2</sup>*NERC Isotope Geosciences Laboratory, British Geological Survey, Nottingham, NG12 5GG, UK*

7 <sup>3</sup>*Geological Survey of Namibia, 1 Aviation Road, Windhoek, Namibia*

8 <sup>4</sup>*Scottish Universities Environmental Research Centre, East Kilbride, G75 0QF, UK*

9

## 10 **ABSTRACT**

11 The end-Cryogenian glaciation (Marinoan) was Earth's last global glaciation yet its duration  
12 and character remain uncertain. Here we report U-Pb zircon ages for two discrete ash beds within  
13 glacial marine deposits from widely separated localities of the Marinoan-equivalent Ghaub Formation  
14 in Namibia:  $639.29 \pm 0.26/0.31/0.75$  Ma and  $635.21 \pm 0.59/0.61/0.92$  Ma. These findings, for the  
15 first time, verify the key prediction of the Snowball Earth hypothesis for the Marinoan glaciation:  
16 longevity, with a duration of  $\geq 4.08 \pm 0.64$  Myr. They also show that glacial sedimentation,  
17 erosion, and at least intermittent open-water conditions occurred 4 million years prior to termination  
18 of the Marinoan glaciation and that the interval of non-glacial conditions between the two  
19 Cryogenian glaciations was 20 Myr or less.

## 20 **INTRODUCTION**

21 The Cryogenian Period (*c.* 720 – 635 Ma) was marked by the two most severe glaciations in  
22 Earth history (Hoffman et al., 1998; Fairchild and Kennedy, 2007), the older Sturtian and younger  
23 Marinoan, and their association with unique lithofacies of cap carbonates (Kennedy et al., 2001;  
24 Hoffman and Schrag, 2002; Hoffman et al., 2011), stable isotope fluctuations (carbon, oxygen,  
25 boron, calcium; Halverson et al., 2005; Kasemann et al., 2005; Bao et al., 2008) and banded iron  
26 formation are evidence for global-scale environmental changes with postulated links to ocean-

27 atmosphere oxygenation and biosphere evolution (Butterfield, 2009; Och and Sjiels-Zhou, 2012;  
28 Sperling et al., 2013). Creation of a unified theory explaining those phenomena, however, has been  
29 hampered by one key obstacle: a lack of temporal constraints. Recently, the Sturtian was shown to  
30 have spanned an astonishing 56 Myr, from about 716 Ma to 660 Ma (Bowring et al., 2007;  
31 Macdonald et al., 2010; Rooney et al., 2014; Rooney et al., 2015). In contrast, the duration of the  
32 Marinoan is unresolved: it terminated at *c.* 635 Ma (Hoffmann et al. 2004; Calver et al., 2004;  
33 Condon et al., 2005; Zhang et al., 2008) but its initiation can only be stated as being younger than  
34 interglacial strata, which in Mongolia have been dated as *c.* 659 Ma (Rooney et al., 2014) and in  
35 China as *c.* 655 Ma (Zhang et al., 2008). Here we report new dates for the Marinoan-equivalent  
36 Ghaub Formation in Namibia that provide a basis for assessing the timing and nature of Earth's last  
37 global glaciation.

#### 38 **GEOLOGY: SAMPLES DW-1 AND NAV-00-2B**

39         The Nosib, Otavi and Mulden Groups comprise the Neoproterozoic sedimentary record of  
40 the Congo craton in northern Namibia (Fig. 1). The Otavi Group (and correlative rocks in the  
41 Swakop Group of the Outjo and Swakop Zones) is a 2-5 km thick carbonate platform-slope-basin  
42 succession formed in the tropics along the margin of the Congo Craton. It is punctuated by two  
43 Cryogenian glacial units (Hoffmann and Prave, 1996; Hofman and Halverson, 2008), the older  
44 Chuos and the younger Ghaub formations and their respective cap carbonates, the Rasthof and  
45 Keilberg formations. U-Pb zircon ages on igneous and volcanic units provide geochronological  
46 constraints (see Fig. 1) that bracket deposition of the glacial-bearing strata in the Otavi Group to  
47 between *c.* 756 Ma and 635 Ma.

48         One of the most informative exposures of the Ghaub Formation in northern Namibia is  
49 along Fransfontein Ridge (Fig. 1). There, the Ghaub rocks vary in thickness from 1 to 600 m and  
50 can be traced continuously for *c.* 70 km; they consist mostly of stratified and massive carbonate-  
51 clast-rich diamictite, minor intervals of rippled and cross-stratified dolomitic grainstone, marl and  
52 shale, and an upper unit, the 1 to 15 m thick Bethanis member (Hoffman and Halverson, 2008)

53 typified by cm- to dcm-thick stratified diamictite and grainstone-mudstone, all with abundant  
54 variably sized dropstones. Detailed studies (Hoffman and Halverson, 2008; Domack and Hoffmann,  
55 2011) of those lithofacies have interpreted them as a succession of moraine and glacimarine  
56 sediments deposited along the margin of a repeatedly advancing and back-stepping ice-grounding  
57 line (Domack and Hoffmann, 2011).

58         Along Fransfontein Ridge, the diamictite-dominated Ghaub Formation contains lenses,  
59 generally a few metres thick, consisting of graded grainstone and laminated to massive calcareous-  
60 dolomitic marl-shale with stringers of dropstones. At Duurwater (Fig. 2) one of these lenses about  
61 15 m below the base of the Keilberg cap dolostone contains a prominent ash bed, sampled as DW-1  
62 (Fig. 3). The DW-1 is the middle of three ash beds; it is 0.18 m thick, pale tan to pale yellow in  
63 colour, characterised by sharp upper and lower contacts, displays a slight fining-upward grading,  
64 contains rare disseminated quartz spar crystals and is overlain and underlain by IRD beds (Fig. 4A).  
65 These features indicate that this bed is an air-fall tuff contemporaneous with deposition of the  
66 glacimarine sediments, hence its age would also be the age of sedimentation for this part of the  
67 Ghaub Formation. Below the DW-1 ash bed is 10-15m of massive diamictite and then a more than  
68 100-m-thick succession of carbonate rhythmite, breccia, laminated marl and shale with dispersed  
69 dropstones and isolated metre-scale and larger blocks derived from pre-Ghaub formation units.  
70 These lithofacies fill a steep-sided incision cut into the pre-Ghaub stratigraphy (Figs. 2, 3); in places  
71 along the Fransfontein outcrop belt as much as 300 m of strata have been cut out along this surface.

72         Sample NAV-00-2B comes from an ash bed in the basinal equivalent of the Ghaub  
73 Formation *c.* 30 m below the contact with the Keilberg cap dolostone at Navachab in central  
74 Namibia (Fig. 3). This occurrence was reported by Hoffman et al. (2004) and readers are referred to  
75 that paper for details.

## 76 **METHODS AND RESULTS**

77         All zircon dates in this study were obtained using established chemical abrasion (CA)  
78 isotope dilution thermal ionisation mass spectrometry (ID-TIMS) methods at the NERC Isotope

79 Geoscience Laboratory of the British Geological Survey (Noble et al., 2015; see Data Repository  
80 for details). U-Pb dates have been determined relative to the gravimetrically calibrated  
81 EARTHTIME mixed U/Pb tracers (Condon et al., 2015; McLean et al., 2015) and  $^{238}\text{U}$  and  $^{235}\text{U}$   
82 decay constants (Jaffey et al., 1971; Mattinson, 2010).

83 Sample DW-1 yielded a population of zircons with a consistent morphology (aspect ratio ~2  
84 and long axis typically 200 to 300  $\mu\text{m}$ ) and colour. Ten zircons were dated by CA-ID-TIMS; U-Pb  
85 data for each analysis are concordant when the uncertainty in the  $^{238}\text{U}$  and  $^{235}\text{U}$  decay constants  
86 (Mattinson, 2010) are considered (Fig. 4B; Data Repository Table 1). All analyses yield a weighted-  
87 mean  $^{207}\text{Pb}/^{206}\text{Pb}$  date of  $639.1 \pm 1.7/1.8/5.0$  (n=10, MSWD=1.08). Of those, one analysis has  
88 dispersion beyond that expected due to analytical scatter (see Data Repository) and is an obvious  
89 outlier with a U-Pb date younger than the main population. Excepting this grain, the other nine  
90 analyses yield a weighted mean  $^{206}\text{Pb}/^{238}\text{U}$  date of  $639.29 \pm 0.26/0.31/0.75$  Ma (95% confidence  
91 interval, n=9, MSWD=2.6), which we interpret as the age of deposition.

92 Sample NAV-00-2B is an aliquot of the sample dated previously as  $635.5 \pm 1.2$  Ma  
93 (Hoffmann et al., 2004) at the Massachusetts Institute of Technology. Re-analysis of this sample  
94 was done to capitalise on the use of CA for the effective elimination of Pb-loss (Mattinson, 2005)  
95 and the EARTHTIME tracer and its comprehensive gravimetric calibration and uncertainty model  
96 (Condon et al., 2015; McLean et al., 2015). The  $^{206}\text{Pb}/^{238}\text{U}$  date for NAV-00-2B derived in this  
97 study is  $635.21 \pm 0.59/0.61/0.92$  Ma (95% confidence interval, n=5, MSWD=3.4; Fig. 4B, Data  
98 Repository Table 2). This date is based upon a subset of the analyses (as explained in the Data  
99 Repository) and, even given improved analytical precision and accuracy, is indistinguishable from  
100 the date published in Hoffmann et al. (2004).

## 101 **DISCUSSION**

102 The  $639.29 \pm 0.26/0.31/0.75$  Ma age for the DW-1 ash bed at Duurwater and the revised age  
103 of  $635.21 \pm 0.59/0.61/0.92$  Ma for the NAV-00-2B ash bed at Navachab now, for the first time,  
104 confirm that the Marinoan glaciation was long-lived, lasting at least  $4.08 \pm 0.64$  Myr. This verifies

105 the key prediction of the Snowball Earth hypothesis for a long duration glaciation. The revised age  
106 for NAV-00-2B also refines and reconfirms that the timing of termination of the Marinoan  
107 glaciation was synchronous worldwide (*i.e.* within error of the age data), occurring between  $635.21$   
108  $\pm 0.59/0.61/0.92$  Ma and  $635.2 \pm 0.5$  Ma, the age of an ash bed in the lower part of the cap  
109 carbonate sequence in China (Condon et al., 2005); a conclusion reinforced by the U-Pb zircon age  
110 of  $636.41 \pm 0.45$  Ma for a volcanoclastic unit in the glacial-cap carbonate transition in Tasmania  
111 (Calver et al., 2004).

112 Since the debut of the Snowball Earth hypothesis, debate has ensued regarding the extent of  
113 land and sea ice during Cryogenian glaciations, the causes of repetitive patterns of inferred  
114 proximal-distal and advance-retreat deposits, and the overall timing and duration of glacial  
115 sedimentation (*e.g.* see discussion by Spence et al., 2016, and references therein). Further, the lack  
116 of well-defined age models has led to an array of climate state and sedimentation scenarios, ranging  
117 from surmising that the Marinoan rock record formed by glacial-interglacial-scale epochs (*e.g.*  
118 Allen and Etienne, 2008; LeHeron et al., 2011) to interpretations of the bulk of that record as  
119 having been deposited during a brief interval of time near to the end of the glacial state (*e.g.* Benn et  
120 al., 2015). Although these interpretations are not necessarily mutually exclusive, assessing them  
121 remains speculative because of the lack of constraints for the absolute timing of sedimentation. Our  
122 new geochronological data provide a better temporal framework for understanding the Marinoan  
123 glaciation. For example, the *c.* 639 Ma DW-1 ash bed occurring above a *c.* 100-m-thick glacimarine  
124 succession shows that glacial erosion and sediment accumulation concurrent with at least  
125 intermittent open-water conditions in the tropics existed more than 4 million years before the  
126 ultimate meltback phase of the Marinoan ice sheets. This impacts on a range of issues regarding the  
127 Marinoan climate state: it provides constraints and corroboration of models that yield results  
128 consistent with such conditions, including predictions of plausible CO<sub>2</sub> levels permissive of  
129 enabling ice-line migration and associated sedimentation in the tropics, as documented for the  
130 Ghaub Formation (*e.g.* Domack and Hoffman, 2011), to considerations of low-latitude *refugia* and

131 the survival of eukaryotic organisms within the main phase of the Marinoan glaciation. Further,  
132 given our new age that provides a minimum duration for the Marinoan glaciation and the *c.* 660 Ma  
133 age for the end of the older Cryogenian glaciation (Sturtian), the intervening interglacial interval  
134 and associated biogeochemical and isotopic events represent a timespan of 20 Myr or less (Fig. 4C).  
135 Determining how and why this period of non-glacial conditions punctuated an otherwise apparently  
136 consistently and largely ice-covered Earth poses an intriguing research question.

137

## 138 **CONCLUSION**

139 The  $639.1 \pm 1.7/1.8/5.0$  Ma age obtained on an ash bed in glacial marine sediments of the  
140 Marinoan-equivalent Ghaub Formation in northern Namibia combined with a refined age of  $635.21$   
141  $\pm 0.59/0.61/0.92$  Ma for an ash bed in the basinal equivalent of the Ghaub Formation in central  
142 Namibia confirm that the Marinoan glaciation was long-lived, at least 4 Myr in duration, and that  
143 the preceding interval of non-glacial conditions was less than 20 Myr in duration. Our data also  
144 confirm that the sedimentary archive of the Marinoan glaciation records glacial erosion-  
145 sedimentation and at least intermittent open-water conditions as much as 4 million years prior to  
146 terminal meltback at *c.* 635 Ma.

147

## 148 **ACKNOWLEDGMENTS**

149 This work was supported by NERC Isotope Geoscience Facility Steering Committee grant  
150 IP-1462-0514. Sincere thanks are extended to the Geological Survey of Namibia for their logistical  
151 support.

152

## 153 **REFERENCES CITED**

154 Allen, P.A., and Etienne, J.L., 2008, Sedimentary challenge to Snowball Earth: *Nature Geosciences*,  
155 v. 1, p. 817-825.

156 Bao, H., Lyons, J.R., and Zhou, C., 2008, Triple oxygen isotope evidence for elevated CO<sub>2</sub> levels  
157 after a Neoproterozoic glaciation: *Nature*, v. 453, p. 504-506.

158 Benn, D.I., Le Hir, G., Bai, H., Donnadieu, Y., Dumas, C., Fleming, E.J., Hambrey, M.J.,  
159 McMillan, E.A., Petronis, M.S., Ramstein, G., Stevenson, C.T.E., Wynn, P.M., Fairchild, I.J.,  
160 2015, Orbitally forced ice sheet fluctuations during the Marinoan Snowball Earth glaciation:  
161 *Nature Geoscience*, v. 8, p. 704-707.

162 Bowring, S.A., Grotzinger, J.P., Condon, J., Ramezani, J., Newall, M.J., and Allen, P.A., 2007,  
163 Geochronologic constraints of the chronostratigraphic framework of the Neoproterozoic Huqf  
164 Supergroup, Sultanate of Oman: *American Journal of Science*, v. 307, p. 1097-1145.

165 Butterfield, N.J., 2009, Oxygen, animals and oceanic ventilation: an alternative view: *Geobiology*,  
166 v. 7, p. 1-7.

167 Calver, C.R., Black, L.P., Everard, J.L., and Seymour, D.B., 2004, U-Pb zircon age constraints on  
168 late Neoproterozoic glaciation in Tasmania: *Geology*, v. 32, p. 893-896.

169 Condon, D.J., Schoene, B., McLean, N.M., Bowring, S.A., and Parrish, R.R., 2015, Metrology and  
170 traceability of U-Pb isotope dilution geochronology (EARTHTIME Tracer Calibration Part I):  
171 *Geochimica et Cosmochimica Acta*, v. 164, p. 464-480,

172 Condon, D., Zhu, M., Bowring, S., Wang, W., Yang, A., and Jin, Y., 2005, U-Pb ages from the  
173 Neoproterozoic Doushantuo formation, China: *Science*, v. 308, p. 95-98.

174 Cox, G.M., Strauss, J.V., Halverson, G.P., Schmitz, M.D., McClelland, W.C., Stevenson, R.S., and  
175 Macdonald, F.A., 2015, Kikiktat volcanics of Arctic Alaska – melting of harzburgitic mantle  
176 associated with the Franklin large igneous province: *Lithosphere* L435-1. DOI:  
177 10.1130/L435.1.

178 Domack, E.W., and Hoffman, P.F., 2011, An ice grounding-line wedge from the Ghaub glaciation  
179 (635 Ma) on the distal foreslope of the Otavi carbonate platform, Namibia, and its bearing on  
180 the snowball Earth hypothesis: *Geological Society of America Bulletin*, v. 123, p. 1448-1477.

181 Fairchild, I.J., and Kennedy, M.J., 2007, Neoproterozoic glaciation in the Earth System: Journal of  
182 the Geological Society, v. 164, p. 895-921.

183 Halverson, G.P., Hoffman, P.F., Schrag, D.P., Maloof, A.C., and Rice, A.H.N., 2005, Toward a  
184 Neoproterozoic composite carbon-isotope record: Geological Society of America Bulletin, v.  
185 117, p. 1181-1207.

186 Hoffman, P.F., 2011, Strange bedfellows: glacial diamictite and cap carbonate from the Marinoan  
187 (635 Ma) glaciation in Namibia: *Sedimentology*, v. 58, p. 57-119.

188 Hoffman, P.F., and Halverson, G.P., 2008, Otavi Group of the western Northern Platform, the  
189 eastern Kaoko Zone and the Northern Margin Zone, in Miller, R.McG., ed., *The Geology of*  
190 *Namibia: Volume 2 Neoproterozoic to Lower Palaeozoic*: Ministry of Mines and Energy,  
191 Namibia, p. 13-69–13-136.

192 Hoffman, P.F., Hawkins, D.P., Isachsen, C.E., and Bowring, S.A., 1996, Precise U-Pb zircon ages  
193 for early Damaran magmatism in the Summas Mountains and Weltwischia Inlier, northern  
194 Damara Belt, Namibia. *Communications of the Geological Survey of Namibia* 11, 47-52.

195 Hoffman, P.F., Kaufman, A.J., Halverson, G.P., and Schrag, D.P., 1998, A Neoproterozoic  
196 snowball Earth: *Science*, v. 281, p. 1342-1346.

197 Hoffman, P.F., and Schrag, D.P., 2002, The snowball Earth hypothesis: testing the limits of global  
198 change: *Terra Nova*, v. 14, p. 129-155.

199 Hoffmann, K.H., Condon, D., Bowring, S., and Crowley, J., 2004, U-Pb zircon date from the  
200 Neoproterozoic Ghaub Formation, Namibia: constraints on Marinoan glaciation: *Geology*, v.  
201 32, p. 817-821.

202 Hoffmann, K.H., and Prave, A.R., 1996, A preliminary note on a revised subdivision and regional  
203 correlation of the Otavi Group based on glacial diamictites and associated cap dolostones:  
204 *Communications of the Geological Survey of Namibia*, v. 11, p. 77-82.

205 Jaffey, A.H., Flynn, K.F., Glendenin, L.E., Bentley, W.C., and Essling, A.M., 1971, Precision  
206 measurement of half-lives and specific of  $^{235}\text{U}$  and  $^{238}\text{U}$ : *Physics Reviews C*4, p. 1889-1906.



207 Kasemann, S.A., Hawkesworth, C.J., Prave, A.R., Fallick, A.E., and Pearson, P.N., 2005, Boron  
208 and calcium isotope composition in Neoproterozoic carbonate rocks from Namibia: evidence  
209 for extreme environmental change: *Earth and Planetary Science Letters*, v. 231, p. 73-86.

210 Kennedy, M.J., Christie-Blick, N., and Prave, A.R., 2001, Carbon isotopic composition of  
211 Neoproterozoic glacial carbonates as a test of paleoceanographic models for snowball Earth  
212 phenomena: *Geology*, v. 29, p. 1135-1138.

213 Lan, Z., Li, X., Zhang, Q., Zhu, M., Chen, Z-Q., Zhang, Q., Li, Q., Lu, D., Liu, Y., and Tang, G.,  
214 2014, A rapid and synchronous initiation of the wide spread Cryogenian glaciations:  
215 *Precambrian Research*, v. 255, p. 401-411.

216 Le Heron, D.P, Cox, G., Trundley, A., and Collins, A.S., 2011, Two Cryogenian glacial successions  
217 compared: Aspects of the Sturt and Elatina sediment records of South Australia: *Precambrian*  
218 *Research*, v. 186, p. 147-168.

219 Macdonald, F.A., Schmitz, M.D., Crowley, J.L., Roots, C.F., Jones, D.S., Maloof, A.C., Strauss,  
220 J.V., Cohen, P.A., Johnston, D.T., and Schrag, D.P. 2010, Calibrating the Cryogenian:  
221 *Science*, v. 327, p. 1241-1243.

222 Mattinson, J.M., 2005, Zircon U-Pb chemical abrasion ("CA-TIMS") method: Combined annealing  
223 and multi-step partial dissolution analysis for improved precision and accuracy of zircon ages:  
224 *Chemical Geology*, v. 220, p. 47-66.

225 Mattinson, J.M., 2010, Analysis of the relative decay constants of  $^{235}\text{U}$  and  $^{238}\text{U}$  by multi-step CA  
226 TIMS measurements of closed-system natural zircon samples: *Chemical Geology*, v. 275, p.  
227 186-198.

228 McLean, N., Condon, D.J., Schoene, B., and Bowring, S.A., 2015, Evaluating Uncertainties in the  
229 Calibration of Isotopic Reference Materials and Multi-Element Isotopic Tracers  
230 (EARTHTIME Tracer Calibration Part II): *Geochimica et Cosmochimica Acta*, v. 164, p.  
231 481-501.

232 Miller, R. McG., 2008, The Geology of Namibia: Neoproterozoic to lower Palaeozoic. Ministry of  
233 Mines and Energy, Geological Survey, Namibia.

234 Noble, S.R., Condon, D.J., Carney, J.N., Wilby, P.R., Pharoah, T.C., and Ford, T.D., 2015, U-Pb  
235 geochronology and global context of the Charnian Supergroup, UK: Constraints on age of key  
236 Ediacaran fossil assemblages. Geological Society of America Bulletin, v. 127, p. 250-265.

237 Och, L.M. & Shields-Zhou, G.A., 2012, The Neoproterozoic oxygenation event: Environmental  
238 perturbations and biogeochemical cycling: Earth-Science Reviews, v. 110, p. 26-57.

239 Rooney, A.D., Macdonald, F.A., Strauss, J.V., Dudás, F.Ö., Hallmann, C., and Selby, D., 2014, Re-  
240 Os geochronology and coupled Os-Sr isotope constraints on the Sturtian snowball Earth:  
241 Proceedings of the National Academy of Sciences, v. 111, p. 51-56.

242 Rooney, A.D., Strauss, J.V., Brandon, A.D., and Macdonald, F.A., 2015, A Cryogenian  
243 chronology: Two long-lasting synchronous Neoproterozoic glaciations: Geology, v. 43, p.  
244 459-462.

245 Spence, G.H., Le Heron, D.P., and Fairchild, I.J., 2016, Sedimentological perspectives on climatic,  
246 atmospheric and environmental change in the Neoproterozoic Era: Sedimentology, v. 63, p.  
247 253-306.

248 Sperling, E.A., Halverson, G.P., Knoll, A.H., Macdonald, F.A., and Johnston, D.T., 2013, A basin  
249 redox transect at the dawn of animal life: Earth and Planetary Science Letters, v. 371-372, p.  
250 143-155.

251 Zhang, S., Jiang, G., and Han, Y. 2008, The age of the Nantuo Formation and Nantuo glaciation in  
252 South China: Terra Nova, v. 20, p. 289-294.

253 Zhou, C., Tucker, R, Xiao, S., Peng, Z. Yuan, X. and Chen, Z., 2004, New constraints on the ages  
254 of Neoproterozoic glaciations in south China: Geology, v. 32, p. 437-440.

255

256 **Figure 1.** Generalised geologic framework of northern Namibia. Ages for the Naauwpoort  
257 Formation (NF) and Oas Syenite (OS) are from Hoffman et al. (1996), for the Ombombo Subgroup  
258 from Halverson et al. (2005), and for the Ghaub Formation from Hoffmann et al. (2004) and this  
259 paper. Ages of the Damara granitoids from Miller (2008, and references therein).

260

261 **Figure 2.** Fransfontein Ridge geology in the vicinity of sample DW-1. See Figure 1 for location.

262

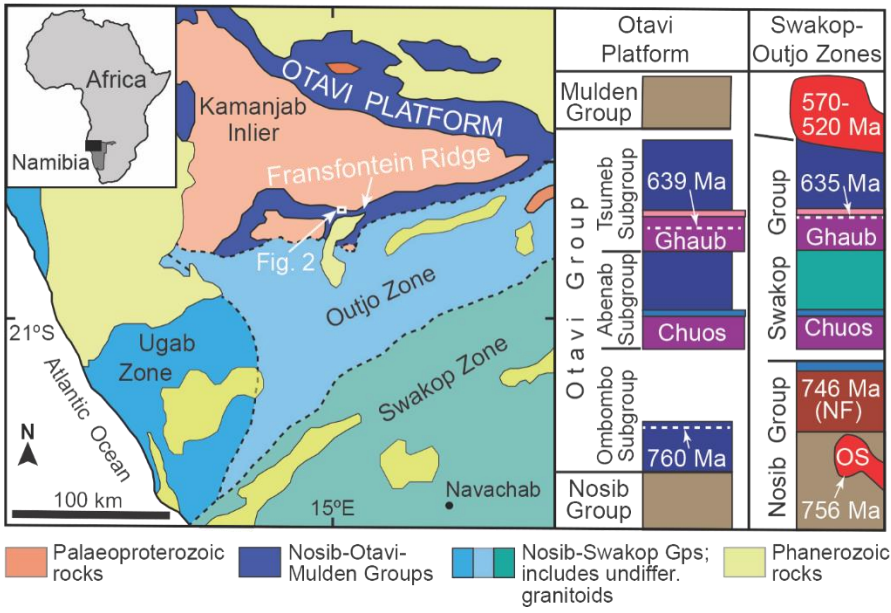
263 **Figure 3.** Simplified stratigraphy of the Fransfontein Ridge area around Duurwater and of the  
264 Navachab area (for details of Navachab see Hoffmann et al., 2004); left column is a detailed section  
265 showing the stratigraphic position of the DW-1 ash bed, the middle of three ash beds, within the  
266 diamictic interval of the Ghaub Formation (sample location: 15.14693E 20.20940S).

267

268 **Figure 4. A.** DW-1 ash bed between ice-rafted-debris beds, Duurwater section. **B.** U-Pb Concordia  
269 plot of data for samples DW-1 and NAV-00-2B; solid ellipses represent analyses included in age  
270 calculation, dashed ellipses are not included (see Data Repository for explanation). **C.**

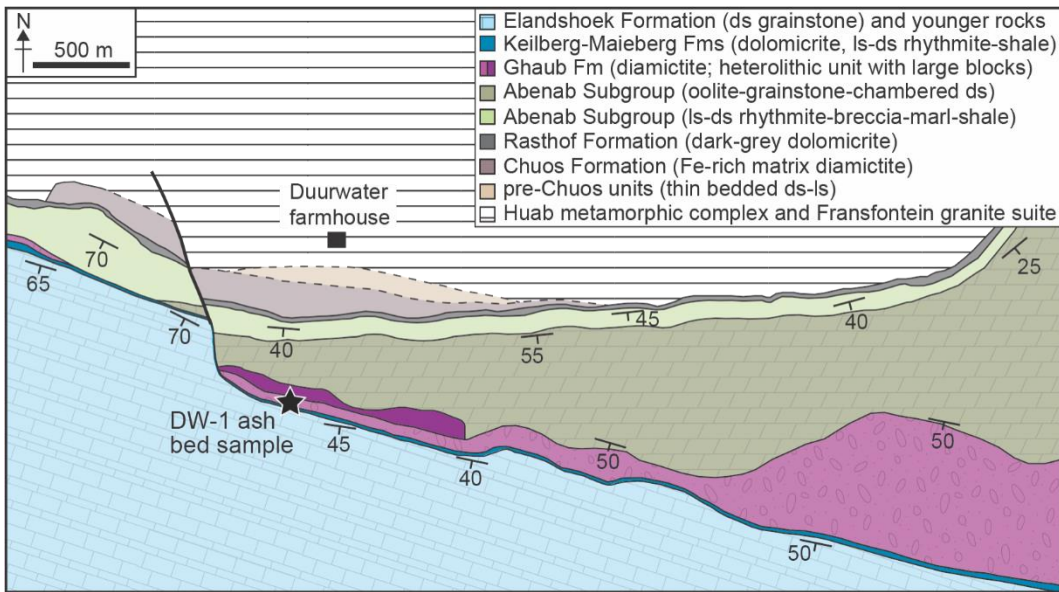
271 Neoproterozoic timeline trends for key isotope proxy datasets: S isotopes after (from Och and  
272 Shields-Zhou, 2012, and references therein); Sr and C isotopes after (Halverson et al., 2005) and  
273 our own data. U-Pb age data from: 1– Lan et al. (2014), 2–Macdonald et al. (2010), 3–Zhou et al.  
274 (2004), 4–Zhang et al. (2008), 5–Condon et al. (2005). Bold ages are reported herein.

275



277

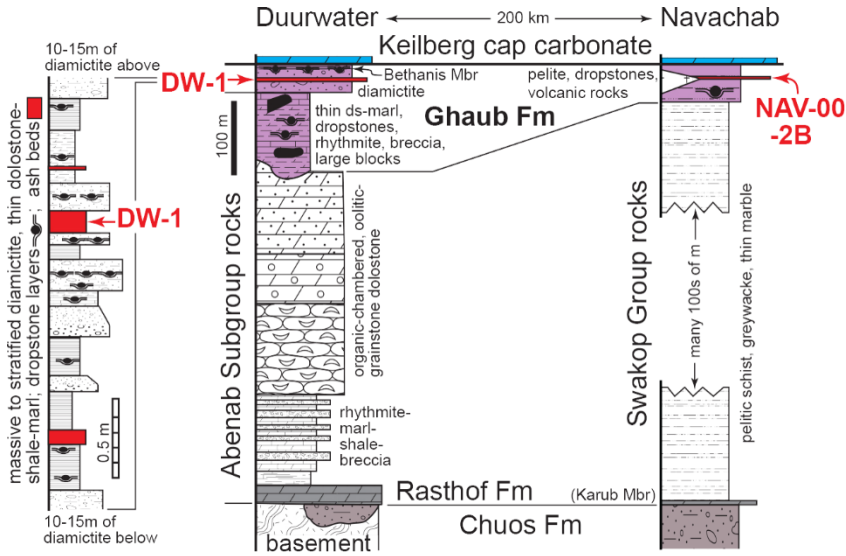
278



280

281

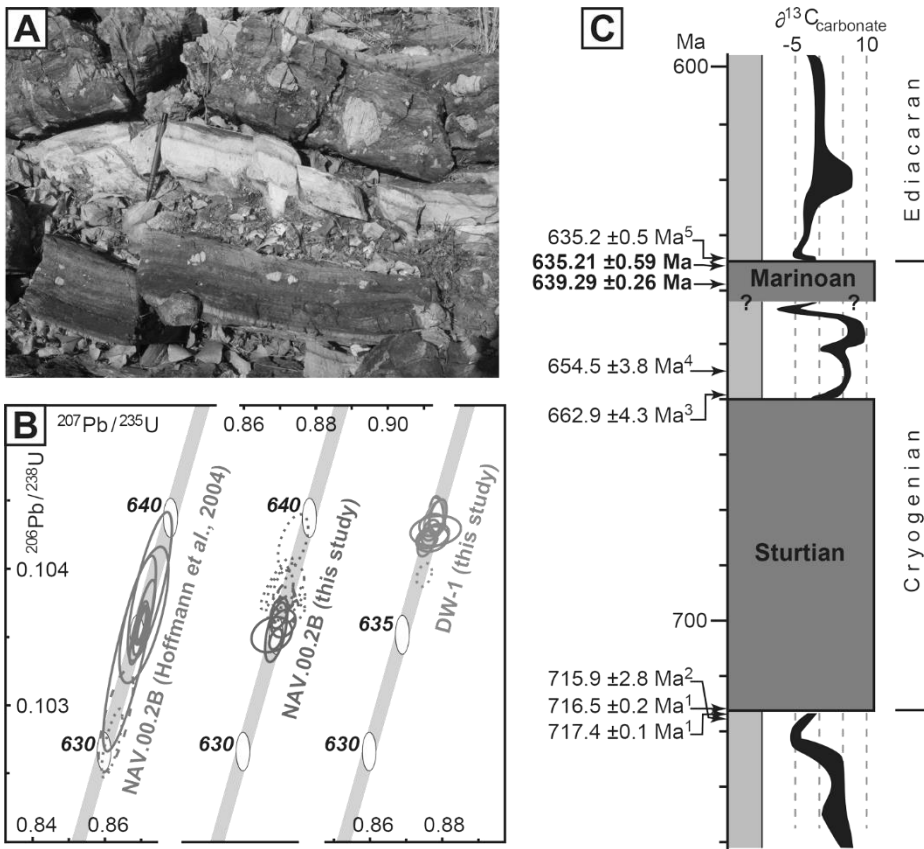
282 Figure 3.



283

284

285 Figure 4.



286